The speed, reflection and intensity of waves propagating in flexible tubes with aneurysm and stenosis: Experimental investigation

Wisam S Hacham[1,2] and Ashraf W Khir[1]

Abstract

A localized stenosis or aneurysm is a discontinuity that presents the pulse wave produced by the contracting heart with a reflection site. However, neither wave speed (c) in these discontinuities nor the size of reflection in relation to the size of the discontinuity has been adequately studied before. Therefore, the aim of this work is to study the propagation of waves traversing flexible tubes in the presence of aneurysm and stenosis in vitro. We manufactured different sized four stenosis and four aneurysm silicone sections, connected one at a time to a flexible 'mother' tube, at the inlet of which a single semi-sinusoidal wave was generated. Pressure and velocity were measured simultaneously 25 cm downstream the inlet of the respective mother tube. The wave speed was measured using the PU-loop method in the mother tube and within each discontinuity using the foot-to-foot technique. The stenosis and aneurysm dimensions and c were used to determine the reflection coefficient (R) at each discontinuity. Wave intensity analysis was used to determine the size of the reflected wave. The reflection coefficient increased with the increase and decrease in the size of the aneurysm and stenosis, respectively. c increased and decreased within stenosis and aneurysms, respectively, compared to that of the mother tube. Stenosis and aneurysm induced backward compression and expansion waves, respectively; the size of which was related to the size of the reflection coefficient at each discontinuity, increases with smaller stenosis and larger aneurysms. Wave speed is inversely proportional to the size of the discontinuity, exponentially increases with smaller stenosis and aneurysms and always higher in the stenosis. The size of the compression and expansion reflected wave depends on the size of R, increases with larger aneurysms and smaller stenosis.

Background

The normal function of the systemic circulation can be disturbed by abnormalities such as stenosis and aneurysms, where localized narrowing or enlargement of the arterial segment is presented. The reflection of waves travelling from the heart towards the periphery is an important consequence of the existence of these discontinuities. These reflected waves are known to increase ventricular mechanical load,[1] and it is therefore desirable to examine and quantify the size of reflections at such discontinuities.

Swillens et al.[2] studied the effect of an abdominal aortic aneurysm on aortic arterial wave reflection. The authors indicated the presence of pronounced reflections in the pressure and flow waveforms in the context of aneurysm. They measured experimentally the reflection coefficient in the upper aorta and stated that it is negative and positive with and without aneurysm, respectively.

Wave intensity analysis (WIA) is a technique that is useful for studying cardiac–arterial interaction and has the benefit of being a time-domain technique.[3] This

[1]Brunel Institute for Bioengineering, Brunel University London, London, UK
[2]University of Baghdad, Baghdad, Iraq

Corresponding author:
Ashraf W Khir, Brunel Institute for Bioengineering, Brunel University London, Uxbridge, Middlesex, London UB8 3PH, UK.
Email: Ashraf.Khir@brunel.ac.uk

method also allows the separation of the measured pressure and velocity waves into their forward and backward directions.[4,5] In essence, wave intensity (dI) is a hemodynamic expression that represents the energy flux carried by the wave per cross-sectional area of the vessel. By definition, dI is calculated as the product of the changes in pressure (dP) and the changes in velocity (dU) across the wavefront. The solution of the one-dimensional (1D) conservation equations of mass and momentum by the method of characteristics for the simultaneous measurements of pressure and velocity is the basis of this time-domain analysis. One of the benefits of WIA is that it allows for the separation of pressure and velocity waveforms into their forward and backward directions, but requires knowledge of the wave speed (c), which can be determined using one of the several techniques such as the traditional foot-to-foot method, pressure–velocity loop (PU-loop),[6] lnDU-loop,[7] or the classical Moens–Korteweg (M–K) equation.[8] In fact, it has been shown that the PU-loop can be used to determine simultaneously both c and the arrival time of the reflected wave.[6]

The nature, shape and magnitude of the arterial pressure waveform are impacted physiologically and clinically with the presence of reflected waves that are generated at reflection sites, which can be expressed by the reflection coefficient (R). It has been shown that the ratios of the wave energy or pressure of the reflected to the incident wave can be used to determine R. Li et al.[9] used wave intensity definition to determine the reflection coefficient. The authors used an in vitro experimental setting with a single inlet flexible tube joined to a second flexible tube with different properties to form a single reflection site. They concluded that the reflection coefficients increased or decreased with distance from the reflection site, depending on the type of reflection site.

The changes in the mechanical properties and dimensions of the arterial lumen usually produce a discontinuity/reflection site. The reflection at a discontinuity with converging wall, a decrease in the arterial lumen, will be positive, and the forward compression wave (FCW) would be reflected as a backward compression wave (BCW). Likewise, the reflection at a discontinuity with a diverging wall, an increase in size of the arterial lumen, will be negative and the FCW will be reflected as a backward expansion wave (BEW). In either case, the reflected waves will be travelling backwards towards the heart, and hence the interest in studying arterial discontinuities such as stenosis and aneurysm and their reflection.

The time for arrival of reflected waves to the aortic root is important physiologically because, when the reflected waves arrive before the closing of the aortic valve, the left ventricle will be required overcome the increase in pressure produced by those reflected waves. The deconvolution of the backward pressure wave can be used to determine the distances to the reflection sites with the aid of time delay between the forward and backward components of the pressure waveform.[10,11] For example, time difference between the pressure upstroke to the pressure at the inflection point, or the arrival of reflected wave as determined by WIA is the time it takes the wave to run forward, be reflected and arrive back, and with knowledge of c the distance to reflection site can be determined.[12]

In this study, we aim to measure (c) within the aneurysm and stenosis, which, as far as the authors are aware, has not been studied before. We also aim to investigate the reflection produced by the aneurysm and stenosis and study the magnitude of reflected wave in relation as a function of the discontinuities: aneurysm and stenosis.

Methods

We quantify the magnitude of the reflected waves resulting from the stenosis and aneurysm using WIA, which is described below. Due to its importance in the analysis, wave speed (c) will be determined at each location using two techniques as an internal measure of consistency.

WIA

The solution of Euler's conservation equations of mass and momentum for the 1D homogeneous, inviscid and incompressible fluid flow in elastic tubes by the method of characteristics is the basis of WIA.[13] Wave intensity (dI) can be defined as the energy carried by the wave per unit area, which has the units of W/m^2 and can be calculated by the following equation

$$dI = dPdU \tag{1}$$

where dP and dU are the changes in pressure (P) and velocity (U) between each two successive sampling periods, respectively. The water hammer equations in the forward (+) and backward (–) directions can be expressed as

$$dP_\pm = \pm \rho c dU_\pm \tag{2}$$

where ρ is the fluid density. If we assume waves interact linearly such that

$$dP = dP_+ + dP_-, \quad dU = dU_+ + dU_- \tag{3}$$

Using equations (2) and (3), dP and dU can be separated into the + and – directions as[3]

$$dP_\pm = \frac{1}{2}\left(dP \pm \rho c dU\right), \quad dU_\pm = \frac{1}{2}\left(dU \pm (dP/\rho c)\right) \tag{4}$$

The pressure and velocity waveforms in the (+) and (−) directions were separated by integrating dP and dU in the (+) and (−) directions

$$P_\pm = P_0 + \sum_{t=0}^{T} dP_\pm, \quad U_\pm = U_0 + \sum_{t=0}^{T} dU_\pm \tag{5}$$
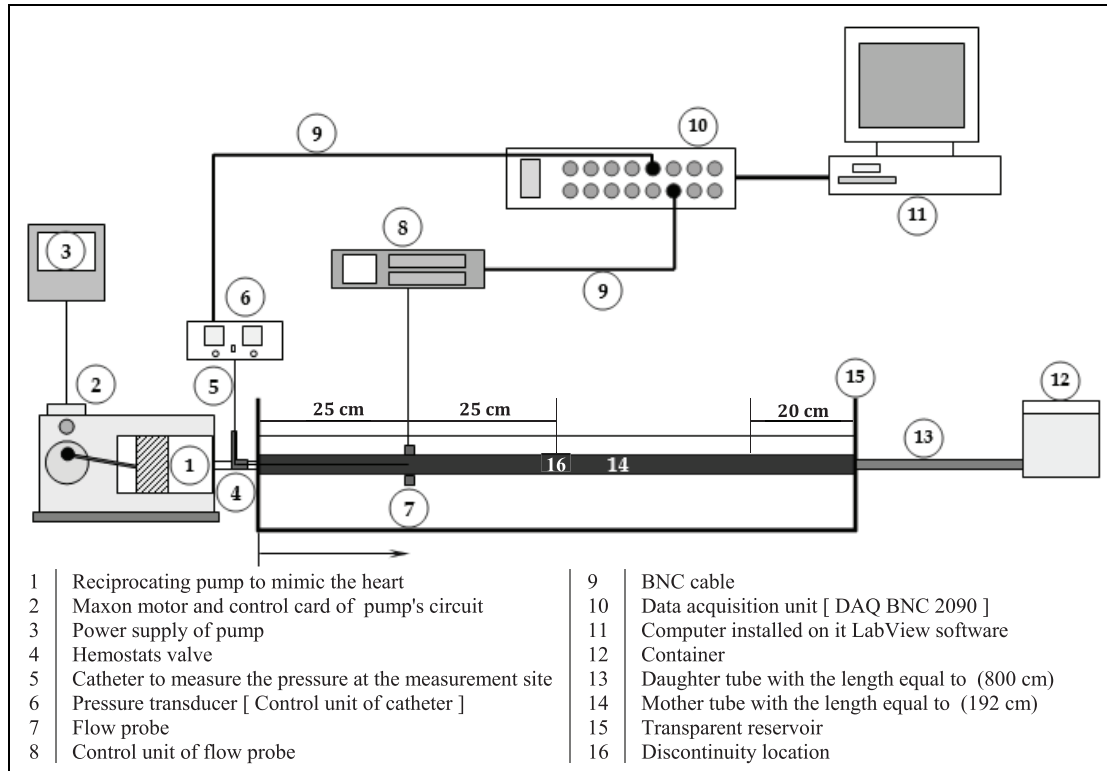
Figure 1. A schematic diagram of the experimental setup including all parts of this construction. Mother and daughter tubes connected in line with the pump and cylindrical reservoir. All elements of the experiment are on the same horizontal platform. The raw indicates the positive flow direction.

where P_0 and U_0 are the integration constants, which are taken arbitrarily as the initial pressure and velocity. T denotes the duration of one cycle. Wave intensity can then be separated into the (+) and (–) directions as follows

$$dI_\pm = \frac{(dP \pm \rho c dU)^2}{4\rho c} \qquad (6)$$

Wave intensity in the forward (+) and backward (–) directions are the energy carried by the forward and backward travelling waves, respectively.

Integrating under the wave intensity curve with respect to time gives the wave energy

$$I_\pm = \int_0^T dI_\pm \qquad (7)$$

Wave speed determination

Foot-to-foot technique (f-t-f). This traditional technique was used to determine wave speed in the mother tube and within each stenosis and aneurysm utilizing pressure transducers. The distance between pressure transducers was 147 cm in the case of the mother tube and 9 and 10 cm in the case of aneurysms and stenosis, respectively, as shown in Figures 1 and 2.

PU-loop method. This technique was originally introduced by Khir et al.[14] and relies on the linear relationship between pressure and velocity in the absence of reflected waves, which can be expressed as

$$c = \pm \frac{1}{\rho}\left(\frac{dP}{dU}\right)_{linear\, portion} \qquad (8)$$

The time lag between pressure and velocity due to the different frequency response of the measurement systems was found to be $\sim$6 ms, which was accounted for before the analysis, using an earlier described technique.[15] This technique was used to double-check results of f-t-f results in the mother tube.

M–K equation. This technique allows calculation of c if information on the mechanical properties of the tube is available.[8] This equation can be written as

$$c = \sqrt{\frac{Eh}{\rho D}} \qquad (9)$$

where h is the wall thickness and D is the uniform inner diameter. This technique was used to double-check results of the f-t-f in the aneurysm and stenosis sections in the in vitro setup.
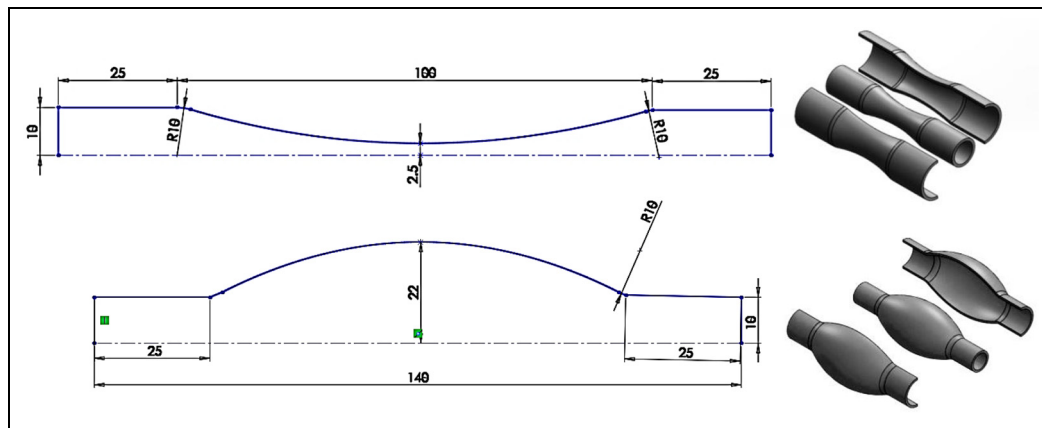
Figure 2. Top panel: drawings for a respective stenosis (left) and the mould configuration (right) for a manufactured stenosis of 10 cm length and 0.5 cm minimum diameter. Bottom panel: technical drawings for a respective aneurysm (left) and the mould configuration (right) for a manufactured aneurysm of 9 cm length and 4.4 cm maximum diameter. All dimensions are in mm.

Wave reflections

When the pulse wave encounters a discontinuity, a reflection is generated. This study deals with the discontinuities as lumen change from the mother lumen area (A_0) to discontinuity lumen area (A_1). Hence, the theoretical reflection coefficient (R_t) can be estimated as

$$R_t = \frac{\left(\frac{A}{c}\right)_0 - \left(\frac{A}{c}\right)_1}{\left(\frac{A}{c}\right)_0 + \left(\frac{A}{c}\right)_1} \qquad (10)$$

where c_0 and c_1 are the wave speed in the mother and discontinuity vessels, respectively.

According to equation (10), R_t will be negative and positive at aneurysm and stenosis, respectively. Furthermore, the reflection at a discontinuity can be determined experimentally using the reflection coefficient as previously described[14]

$$R_{dP} = \frac{dP_-}{dP_+} \qquad (11)$$

where dP_- and dP_+ are the magnitudes of the reflected and incident pressure waveforms as calculated using equation (4).

Another expression for R can also be described using amplitudes of the FCW and BCW of WIA as calculated using equations (6) and (7)

$$R_{dI} = \frac{dI_-}{dI_+} \qquad (12)$$

where dI_- and dI_+ are amplitudes of the reflected and incident wave intensities.

According to wave energy, the reflection coefficient can be calculated by

$$R = \frac{I_-}{I_+} \qquad (13)$$

where I_- and I_+ are the wave intensities due to the reflected wave and incident wave, respectively.

Experimental set-up

The experimental setup is illustrated in Figure 1. The main elements are described below.

Reciprocating pump. Reciprocating pump is connected to a piston pump that is driven by a scotch yoke run using an electric motor (Maxon, DC-Max, Switzerland), which is supplied by AC 12 V. An approximately half-sinusoidal, single pulse at frequency 1.1 Hz, in the forward direction, was generated in all the experiments. The volume of water injected was approximately 40 cc over a duration of 0.9 s.

Elastic tubes. The mother tube has a uniform circular cross-sectional area along its 192 cm length, uniform wall thickness of 0.2 cm, and inner diameter of 1.7 cm. The daughter tube is 4 m in length, with a uniform lumen diameter of 1 cm and wall thickness of 0.2 cm. The elastic tubes are made of silicone rubber (Health Care, London, UK).

Reservoirs. Two reservoirs were used, one of which, mounted downstream and direct to pump of system, was used to include the mother tube, while the other was placed downstream of the daughter tube to containment and compensate the amount of water during the compression and retracting course for the pump piston, respectively.

Measurements. Transducer-tipped catheters (Gaeltec, Scotland, UK) have been used to measure the pressure at 25 cm downstream the inlet of the mother tube and at 20 cm upstream the outlet of the mother tube – distance between the two transducers is 147 cm. The fluid flow velocity was measured using ultrasound flow meter and probes (HT323; Transonic, NY, USA). The simultaneous pressure and flow measurements were taken at 25 cm away from the inlet of the mother tube. National

Instruments (BNC-2090 DAQ, TX, USA) system was used to sample the data using LabView at a rate of 500 Hz. Home-written programmes in MATLAB software were used for the analysis of the data, offline.

Discontinuities. Eight silicone rubber parts were manufactured; four to mimic aneurysms and four to mimic stenosis. These parts were assembled into the respective mother rubber tube. The maximum inner diameters of the aneurysms were 2.4, 3.4, 4.4 and 5 cm, while the minimum inner diameters of the stenosis parts were 1.3, 1.0, 0.5 and 0.25 cm. All discontinuities have wall thickness of 0.2 cm, and tensile testing indicated Young's modulus of 1.3 MPa. Each discontinuity joined the mother tube at 50 cm away from the inlet. The discontinuities were manufactured using three-dimensional (3D) printing. Liquid silicone (98%) and easy composites *CS2* catalyst (2%) to solidify the liquid silicone material were mixed and injected into the moulds to form the artificial silicone rubber parts to mimic the aneurysms and stenosis (Figure 2). The size and shape of aneurysm and stenosis are based on the studies by Pape et al.[16] and Chambers,[17] respectively, which have also been used in our earlier work.[18]

Tensile testing. Estimation of the Young's modulus of elasticity (E) provides a possibility to calculate the wave speed by employing the M–K equation. We measured (E) of our mother tube and discontinuities (aneurysms and stenosis) using tensile testing (Instron High Wycombe, UK) with a matching servo load cell. The relation between the extension and the load applied was established using Instron software (Bluehill2) and Young's modulus was found to be 3.3 and 1.3 MPa for the mother tube and discontinuities, respectively.

Results

The pressure and velocity waveform propagation through the lumens and their established reflections from the sudden change in geometry were characterized to wave abnormality due to the context of discontinuity, where the measurement was taken at 25 cm downstream of the mother tube inlet.

Wave speed of mother tube

Wave speed was measured in the mother tube without inclusion of the aneurysm or stenosis (*control*) using the PU-loop technique and found to be 20 ± 0.25 m/s. To confirm this wave speed, we also used the f-t-f method.

The distance between the two measurement sites is 147 cm, and the time of flight is 0.0735 s. Therefore, wave speed of the mother tube according to the f-t-f technique is also 20 ± 0.35 m/s.

Wave speed within the aneurysms and stenosis

Wave speed was measured through the stenosis and aneurysm using the f-t-f technique, and the results are included in Table 1. The data were collected at the inlet and outlet of the discontinuities. Wave speed decreased exponentially with the increase in the centre point of the aneurysm (Figure 3). Also, the M–K equation (9) was also used to verify the results of the f-t-f technique, which required measurements of Young's modulus and wall thickness. These were measured and found to be 1.3 MPa and 2 mm, respectively. In using this equation, we considered the internal diameter of each discontinuity as reported in Table 1, and the density of the fluid (water) is 1000 kg/m^3. The relations between the discontinuity size and wave speed within the stenosis and aneurysm are ($Y = -12.299X + 29.878$; $R^2 = 0.9569$) and ($Y = -2.7551X + 19.469$; $R^2 = 0.9918$), respectively. Wave speed results using the M–K and f-t-f methods are in good agreement.

Control measurements of pressure, velocity and wave intensity

Figure 4 shows the measured, separated forward and backward, pressure, velocity and wave intensity, simultaneous measurements of pressure and velocity taken at 25 cm downstream of the inlet of the mother tube. It can be observed that the measured and forward

Table 1. Theoretical reflection coefficient (R_t) values due to the stenosis and aneurysm discontinuity.

	ID (cm)	A_1 (m^2)	c_0 (m/s)	$(c_1)_{f\text{-}t\text{-}f}$ (m/s)	$(c_1)_{M–K}$ (m/s)	R_t
Stenosis	0.25	0.4908E–5	20	28	32	0.9696
	0.5	1.9634E–5	20	22	23	0.8542
	1.0	7.8539E–5	20	16	16	0.4446
	1.3	13.273E–5	20	14	14	0.0896
Aneurysm	2.4	4.5238E–4	20	13	10	–0.5081
	3.4	9.0792E–4	20	10	9	–0.7777
	4.4	15.200E–4	20	8	8	–0.9006
	5.0	19.634E–4	20	7	7	–0.9329

c is the wave speed in m/s. The cross-sectional area (A_0) of the mother tube used in equation (10) is equal to 2.2698E–4 m^2. ID is the inner diameter, minimum for stenosis and maximum for aneurysm and A_1 is the cross-sectional area corresponding to each discontinuity. The subscripts f-t-f and M–K indicate foot-to-foot and Moens–Korteweg techniques, respectively, for determining wave speed in discontinuity. c_0 and c_1 are the wave speeds in the mother tube (control) and discontinuities, respectively. c_0 was calculated using the PU-loop technique. Wave speed is higher within the stenosis than the aneurysm.
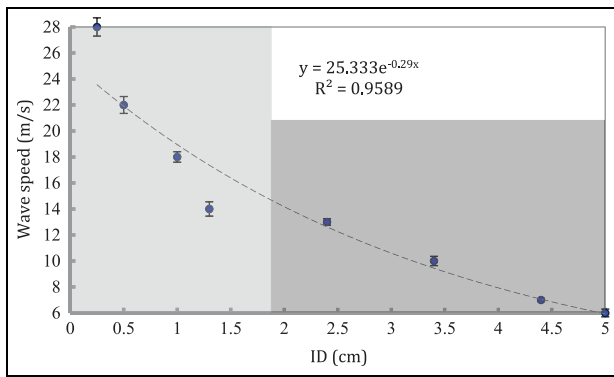ID: inner diameter; f-t-f: foot-to-foot technique; M–K: Moens–Korteweg; PU-loop: pressure–velocity loop.

Figure 3. Effect of the stenosis and aneurysm size on wave speed. ID is the maximum internal diameter of each aneurysm and minimum diameter of each stenosis, which were taken at the centre of each discontinuity. Highlighted in light grey are results of the stenosis and in dark grey are those of the aneurysm discontinuities. Wave speed is higher within the stenosis than the aneurysm. Data are presented as mean of four measurements, and the error bars indicate standard deviation. The dashed curve represents the exponential regression of data, described by the equation and correlation coefficient, $R^2 = 0.95$.

waveforms for dI_-, P_- and U_- are superimposed from the onset of the pulse cycle until the arrival time of reflection (T_R), which is 0.168 s, as indicated by the dashed line.

Effect of aneurysm and stenosis

The aneurysm presented the system with a negative reflection site and generated a BEW. In contrast, the stenosis presented a positive reflection site and generated BCW.

The measured pressure profile and separation into forward and backward waves are shown in Figure 5. The reflected BEWs in the cases of aneurysm had a negative sign (opposite to the FCW that had positive sign). The reflected BCWs in the cases of stenosis maintained the positive sign of the FCW.

Also, the reflected backward expansion velocity waves in the case of aneurysm maintained the positive sign of the forward compression velocity waves, and the reflected backward compression velocity waves in the case of stenosis changed the sign of the waves in the velocity.

Table 2 shows that there is no significant difference between the pattern of WI in 1.0 and 1.3 cm stenosis.

Reflected pressure waveform (P_-) was separated from the incident pressure wave (P_+) using WIA. Figure 6 shows that the reflected pressure wave increased with the increase in size of the aneurysm and with the decrease in the size of the stenosis. The relationship between the reflected wave and the size of aneurysm and stenosis is linear with correlation coefficients of $R^2 = 0.98$ and $R^2 = 0.88$, respectively.

Reflected wave intensities (dI_-) followed a similar pattern to that of the reflected pressure. An increased size of the aneurysm and smaller size of the stenosis resulted in increase in the magnitude of reflected wave
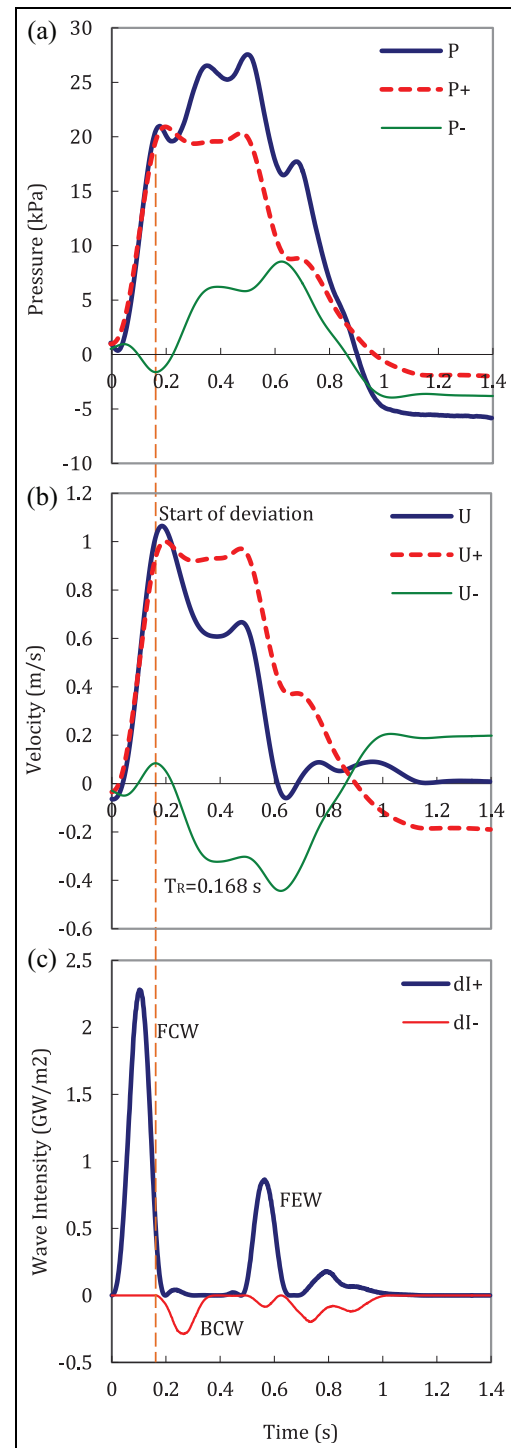

Figure 4. Measured pressure (*P*), velocity (*U*) waveforms and calculated wave intensity (*dI*), and their separation into forward (+) and backward (−) are shown in (a), (b) and (c), respectively. Measurements are taken at (25 cm) downstream of the mother tube inlet without discontinuity. The dashed line indicates the arrival time of reflected wave, $T_R = 0.168$ s, in agreement with the onset of the backward wave intensity (c), and the time of the separated forward and measured pressure (a), forward and measured velocity (b).
FEW: forward expansion wave.

intensity. As shown in Figure 7, the relationship between the reflected intensity and the size of the discontinuity is linear with correlation coefficients of R^2
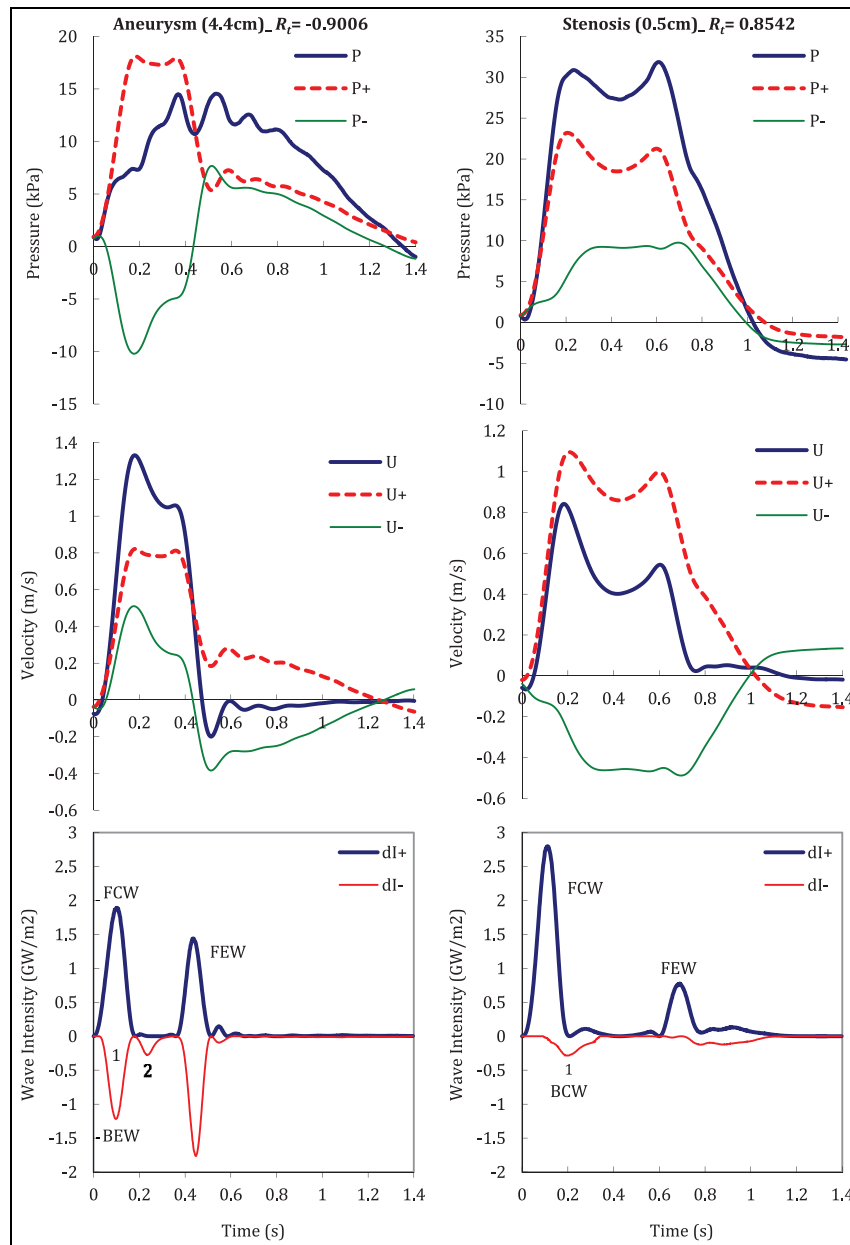
Figure 5. Measured pressure (*P*), velocity (*U*) and calculated wave intensity (*dI*) and their separation into forward (+) and backward (–) directions at 25 cm downstream inlet of the mother tube with the context of 4.4 cm aneurysm (left column) and with the context of 0.5 cm stenosis (right column). R_t is the theoretical reflection coefficient calculated from equation (10).
FEW: forward expansion wave.

= 0.965 and R^2 = 0.859 in the cases of aneurysm and stenosis, respectively.

Theoretical and experimental reflection coefficients

Table 1 includes magnitude of the theoretical reflection coefficient calculated using equation (10), which depended on the measured wave speed through the discontinuities (aneurysm or stenosis) of the in vitro model. The magnitude of *c* within these discontinuities depended largely on the size of the discontinuities. Decreasing size of the stenosis led to increase in the reflection coefficient's values, and oppositely increasing

size of the aneurysms resulted in increasing the reflection coefficient's values. It can be observed that the respective in vitro model produces reflected waves with the reflection coefficients increased with the increase in aneurysm size and the decrease in stenosis size.

Discussion

In this study, we have investigated wave speed within four different sized aneurysms and stenosis and compared the theoretical values based on the M–K equation (9) with those measured experimentally. Also, we studied the effect of these discontinuities on the

Table 2. Time of the wave intensity (*T*), peak wave intensity (*dI*), wave energy (*I*), pressure (*P*) and velocity (*U*) in forward (+) and backward (–) directions as well as wave speed (*c*) through the mother tube and respective aneurysms and stenosis at the 25 cm downstream inlet of the mother tube.

| Parameter	Control ID	Stenosis minimum ID				Aneurysm maximum ID			
	1.7	0.25	0.5	1.0	1.3	2.4	3.4	4.4	5.0
dI_+ (W/m^2) × E + 9	2.2831	3.026	2.79	2.46	2.46	2.19	1.91	1.89	1.74
dI_- (W/m^2) × E + 9	0.2876	0.507	0.28	0.23	0.23	0.65	0.85	1.18	1.27
I_+ (J/m^2) × E + 8	2.027	2.784	2.56	2.14	2.14	1.93	1.75	1.64	1.52
I_- (J/m^2) × E + 8	0.281	0.496	0.19	0.12	0.12	0.47	0.54	0.85	0.86
P_+ (Pa) × E + 4	2.110	2.320	2.32	2.110	2.07	1.96	1.91	1.81	1.79
P_- (Pa) × E + 4	0.897	1.442	0.92	0.974	0.95	0.61	0.73	1.02	1.06
U_+ (m/s)	1.015	1.131	1.095	0.9603	0.960	0.9373	0.8677	0.8217	0.7839
U_- (m/s)	0.4643	0.6728	0.536	0.5022	0.491	0.3148	0.3771	0.5104	0.5323
$c_{mother\ tube}$ (m/s)	20	20	20	20	20	20	20	20	20
$c_{discontinuity}$ (m/s)	18	28	22	18	14	13	10	7	6
R_t	0.444	0.9696	0.8542	0.4446	0.0896	−0.5081	−0.7777	−0.9006	−0.9329
$R_{dI} = dI_-/dI_+$	0.126	0.167	0.10225	0.09406	0.09338	−0.2965	−0.4476	−0.6243	−0.731
$R_I = I_-/I_+$	0.138	0.178	0.0759	0.0573	0.0568	−0.2435	−0.3091	−0.5181	−0.563
$R_P = P_-/P_+$	0.425	0.621	0.3965	0.4616	0.4589	−0.3097	−0.3821	−0.564	−0.592

ID: inner diameter (cm).
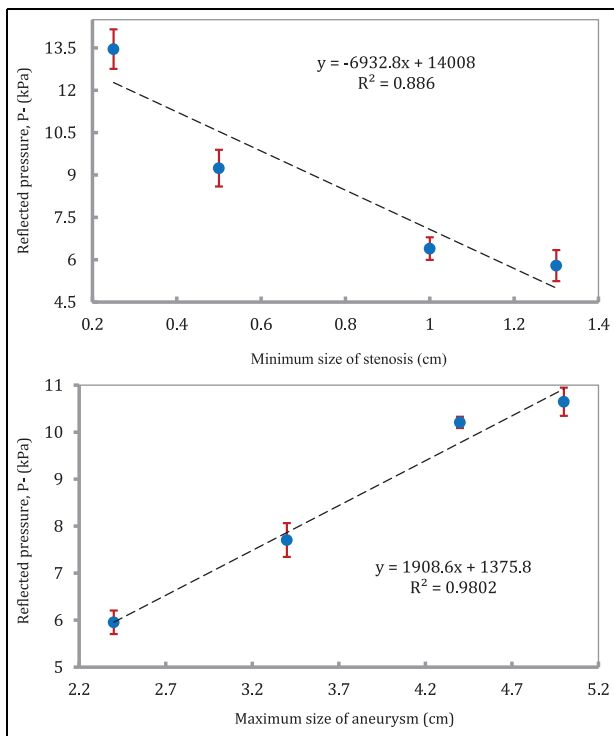
Figure 6. Maximum amplitude of the reflected pressure waveform is plotted against the respective sizes of the discontinuities. Top is the impact of stenosis and lower is the impact of aneurysm. Data are presented as mean of four measurements, and the error bars indicate standard deviation. The dashed lines represent the linear regression of data, described by the equation and correlation coefficient, R^2 = 0.9802.

Figure 7. Maximum amplitude of the reflected wave intensity is plotted against the respective sizes of the discontinuities. Top is the impact of stenosis and lower is the impact of aneurysm. Data are presented as mean of four measurements, and the error bars indicate standard deviation. The dashed lines represent the linear regression of data, described by the equations and correlation coefficients, R^2 = 0.8594 for stenosis and R^2 = 0.9652 for aneurysm.

reflected waves, compared to the theoretical values of the reflection coefficients resulting from the inclusion of the discontinuities with those measured experimentally using WIA. Our main results are that wave speed
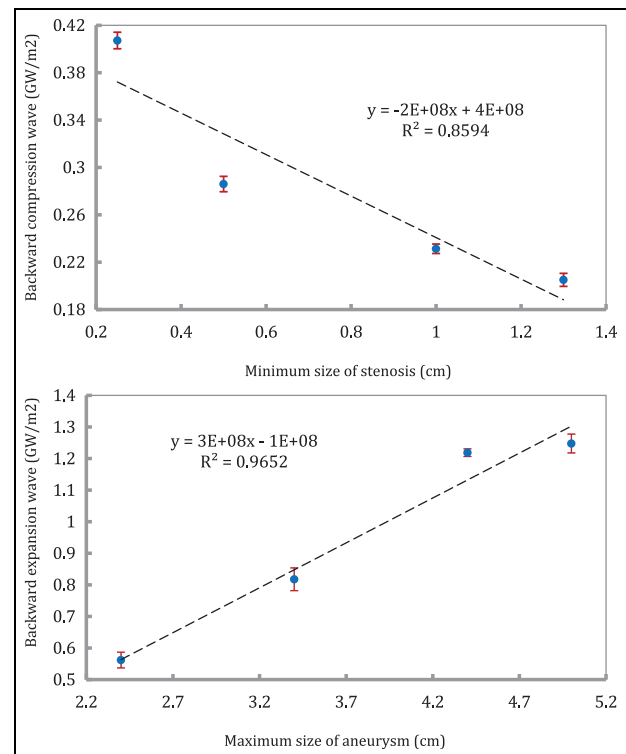
increased and decreased in stenosis and aneurysms, respectively. Furthermore, aneurysm discontinuities caused a reflected expansion, whereas stenosis caused reflected compression waves. The size of the reflected

waves was estimated using the ratio of backward to forward pressure (equation (11)) and backward to forward wave intensity (equations (12) and (13)). Of all causes, the size of the discontinuity highly correlated with the size of the respective reflected wave.

Our results show that wave speed measured experimentally was in good agreement with that estimated using the M–K equation (9) in all our discontinuities. In order to investigate the effect of the discontinuity size on the speed of the wave, all discontinuities were made of the same material and wall thickness. An increase in the maximum inner diameter of the aneurysms caused a decrease in the wave speed in aneurysms, whereas a decrease in the minimum inner diameter of the stenosis resulted in an increase in the wave speed value within those discontinuities. Figure 3 shows the relation between the wave speed and the size of the discontinuity, which in our experiments is evidently linear in the range tested with high correlation coefficients.

According to the theory of wave propagation, the size of the reflected wave is calculated as the product of the size of the incident wave and the reflection coefficient, $dP_- = R_{dp} dP_+$. Since the reflection coefficient varies between 1 (closed end) and –1 (open end), $1 < R > -1$, a forward compression pressure wave is expected to be reflected as a backward compression or expansion wave depending on the sign of the reflection coefficient – compression when $R > 0$ and expansion when $R < 0$. Our experimental results are in line with the theoretical expectations and also with findings of other investigators.[2] In the context of the aneurysms in our experiments, the reflected waves are BEWs (negative reflection), as confirmed by Swillens et al.,[2] while reflections in the context of stenosis are BCWs (positive reflection). A larger aneurysm and a smaller stenosis generate greater reflections.

Figure 5 shows the forward and backward wave intensity, pressure and velocity waveforms calculated from the simultaneous measurements of pressure and velocity, using the WIA, taken at 25 cm downstream the inlet of the mother tube. The results show the influence of the discontinuity on the intensity of the travelling pulse wave. The measured and forward waveforms are superimposed from the onset of the pulse cycle until the arrival time of reflection (T_R), when the forward and measured waveforms begin to deviate from each other. T_R is 0.024 s and indicated by the dashed line representative onset of (dI_-), (P_-) and (U_-). Given the reflection site (aneurysm or stenosis) is 25 cm away from the measurement site, and wave speed in the mother tube of 20 ± 0.25 m/s, the theoretical time to arrive the reflected wave is 0.025 s. This reinforces the experimental results of this study and shows the ability of the wave intensity to capture the arrival timing of the reflected waves.

The wave reflections and their timing have been studied using WIA in vitro,[19] in the carotid artery,[20] in aorta[6,21] and in the coronary arteries.[22] Furthermore, the ratio of negative to positive wave intensity peaks has been used in vivo to derive a reflection *index* in the carotid artery,[23] brachial artery[24] and femoral artery.[5] A fundamental difference between the results presented in this study and those presented in the aforementioned in vivo studies[25] is that the in vitro reflection coefficient values were determined using a single reflection arriving from a single discontinuity, whereas the reflection index in vivo is determined based on multireflections generated along the arterial tree that would include multiple reflection sites. Therefore, the reflection coefficient measured in vitro in this study can be compared with the theoretical reflection coefficient; however, the reflection index measured in vivo should be understood as an index that describes the global reflection phenomenon resulting from a multibranching system.

Limitations

The flexible tubes used in this study are far longer than those available in most mammals and certainly average humans. Also, the tubes used in the current experiments are stiffer than in vivo vessels. However, the main aim of this study was to better understand the speed of waves within discontinuities similar to those present in vivo, and how their size may affect the size of reflections. To achieve this end, a single isolated pulse was needed, which inevitably also required such long tubes, otherwise re-reflected waves would have obscured the fundamental reflection phenomenon. Building on the obtained results and understanding, studying shorter flexible tubes comparable to those of the human body is our next step.

The material of the mother tube is different from that of the stenosis and aneurysms, with different Young's modulus. However, we have calculated the reflection coefficient at each discontinuity based on the inner diameter and wave speed. Therefore, we do not expect this experimental arrangement to have affected the interpretation of the results or conclusions of this work.

Conclusion

Wave speed is inversely and exponentially proportional to the size of the discontinuity, generally slower in the aneurysms than in the stenosis. The larger the size of the aneurysm, the smaller its wave speed, while the smaller the size of the stenosis, the larger its wave speed.

The size of the reflection coefficient is a function of the characteristic impedance at the discontinuity, which in turn depends on the cross-sectional area and the wave speed of the mother and daughter tubes. The larger the difference between the cross-section area of the mother tube and that at the centre of the discontinuity, the larger the size of the reflection coefficient. The larger the size of the aneurysm, the larger the

amplitude of the BEW, whereas the smaller the size of the stenosis, the larger the amplitude of the BCW.

The current results provide valuable insights into the speed and reflection of waves propagating through stenosis and aneurysm in flexible vessels and warrant further studies and an in vivo investigation to establish the physiological value.

Declaration of conflicting interests

The author(s) declared no potential conflicts of interest with respect to the research, authorship and/or publication of this article.

Funding

The author(s) received no financial support for the research, authorship and/or publication of this article.

ORCID iD

Wisam S Hacham [iD] https://orcid.org/0000-0003-3899-2431

References

1. Chirinos JA and Segers P. Noninvasive evaluation of left ventricular afterload: part 2: arterial pressure-flow and pressure-volume relations in humans. *Hypertension* 2010; 56: 563–570.
2. Swillens A, Lanoye L, De Backer J, et al. Effect of an abdominal aortic aneurysm on wave reflection in the aorta. *IEEE Trans Biomed Eng* 2008; 55(5): 1602–1611.
3. Parker KH and Jones CJH. Forward and backward running waves in the arteries: analysis using the method of characteristics. *J Biomech Eng* 1990; 112: 322–326.
4. Hughes AD and Parker KH. Forward and backward waves in the arterial system: impedance or wave intensity analysis? *Med Biol Eng Comput* 2009; 47: 207–210.
5. Borlotti A, Khir AW, Rietzschel ER, et al. Noninvasive determination of local pulse wave velocity and wave intensity: changes with age and gender in the carotid and femoral arteries of healthy human. *J Appl Physiol* 2012; 113: 727–735.
6. Khir AW and Parker KH. Wave intensity in the ascending aorta: effects of arterial occlusion. *J Biomech* 2005; 38(4): 647–655.
7. Feng J and Khir AW. Determination of wave speed and wave separation in the arteries using diameter and velocity. *J Biomech* 2010; 43: 455–462.
8. Kortweg DJ. Uber die For tpflanzungesgechwindigkeit des Schalles in elastischen Rohern. *Ann Phys Chem* 1878; 5: 525–527.
9. Li Y, Parker KH and Khir AW. Using wave intensity analysis to determine local reflection coefficient in flexible tubes. *J Biomech* 2016; 49: 2709–2717.
10. Sazonov I, Khir AW, Hacham WS, et al. A novel method for non-invasively detecting the severity and location of aortic aneurysms. *Biomech Model Mechanobiol* 2017; 16(4): 1225–1242.

11. Zambanini A, Cunningham SL, Parker KH, et al. Wave-energy patterns in carotid, brachial, and radial arteries: a noninvasive approach using wave-intensity analysis. *Am J Physiol Heart Circ Physiol* 2005; 289: H270–H276.
12. Khir AW, Swalen MJP, Feng J, et al. Simultaneous determination of wave speed and the arrival time of reflected waves using the pressure-velocity loop. *Med Biol Eng Comput* 2007; 45(12): 1201–1210.
13. Parker KH. An introduction to wave intensity analysis. *Med Biol Eng Comput* 2009; 47: 175–188.
14. Khir AW, O'Brien A, Gibbs S, et al. Determination of wave speed and wave separation in the arteries. *J Biomech* 2001; 9: 1145–1155.
15. Swalen MJ and Khir AW. Resolving the time lag between pressure and flow for the determination of local wave speed in elastic tubes and arteries. *J Biomech* 2009; 42(10): 1574–1577.
16. Pape LA, Tsai TT, Isselbacher EM, et al. Aortic diameter ≥ 5.5cm is not a good predictor of type A aortic dissection: observations from the International Registry of Acute Aortic Dissection. *Circulation* 2007; 116: 1120–1127.
17. Chambers JB. Aortic stenosis. *Eur J Echocardiogr* 2009; 10: i1–i19.
18. Hacham WS, Abdulla NN, Al-Ammri AS, et al. Wave speed and reflections proximal to aneurism and stenosis of flexible tubes. In: *Proceedings of the 37th IEEE EMBS international conference*, Milan, Italy, 25–29 August 2015, pp.1009–1012. New York: IEEE.
19. Khir AW and Parker KH. Measurements of wave speed and reflected waves in elastic tubes and bifurcations. *J Biomech* 2002; 35: 775–783.
20. Niki K, Sugawara M, Chang D, et al. A new non-invasive measurement system for wave intensity: evaluation of carotid arterial wave intensity and reproducibility. *Heart Vessel* 2002; 17: 12–21.
21. Koh TW, Pepper JR, De Souza AC, et al. Analysis of wave reflections in the arterial system using wave intensity: a novel method for predicting the timing and amplitude of reflected waves. *Heart Vessel* 1998; 13: 103–113.
22. Davies JE, Whinnett ZI, Francis DP, et al. Evidence of a dominant backward-propagating 'suction' wave responsible for diastolic coronary filling in humans, attenuated in left ventricular hypertrophy. *Circulation* 2006; 113(14): 1768–1778.
23. Manisty C, Zambanini A, Parker KH, et al. Differences in the magnitude of wave reflection account for differential effects of amlodipine- versus atenolol-based regimens on central blood pressure: an Anglo-Scandinavian Cardiac Outcome Trial substudy. *Hypertension* 2009; 54: 724–730.
24. Manisty C, Mayet J, Tapp RJ, et al. Wave reflection predicts cardiovascular events in hypertensive individuals independent of blood pressure and other cardiovascular risk factors: an ASCOT (Anglo-Scandinavian Cardiac Outcome Trial) substudy. *J Am Coll Cardiol* 2010; 56: 24–30.
25. Luo J, Fujikura K, Leslie S, et al. Pulse wave imaging of normal and aneurysmal abdominal aortas in vivo. *IEEE Trans Med Imaging* 2009; 28(4): 477–486.